hep-ph/0211206
CERN–TH/2002-289, DCPT/02/122
IPPP/02/61, LMU 09/02
UMN–TH–2114/02, TPI–MINN–02/43
LC-TH-2002-013

# Precision Analysis of the Lightest MSSM Higgs Boson at Future Colliders

**John Ellis**[1], **Sven Heinemeyer**[2], **Keith A. Olive**[3] and **Georg Weiglein**[4]

[1] *TH Division, CERN, Geneva, Switzerland*

[2] *Institut für theoretische Elementarteilchenphysik, LMU München, Theresienstr. 37, D-80333 München, Germany*

[3] *Theoretical Physics Institute, School of Physics and Astronomy, University of Minnesota, Minneapolis, MN 55455, USA*

[4] *Institute for Particle Physics Phenomenology, University of Durham, Durham DH1 3LE, UK*

## Abstract

We investigate the sensitivity of observables measurable in $e^+e^-$, $\gamma\gamma$ and $\mu^+\mu^-$ collisions for distinguishing the properties of the light neutral $\mathcal{CP}$-even Higgs boson in the minimal supersymmetric extension of the Standard Model (MSSM) from those of a Standard Model (SM) Higgs boson with the same mass. We explore first the available parameter space in the constrained MSSM (CMSSM), with universal soft supersymmetry-breaking parameters, incorporating the most recent direct limits on sparticle and Higgs masses, the indirect constraints from $b \to s\gamma$ and $g_\mu - 2$, and the cosmological relic density $\Omega_\chi h^2$. We calculate the products of the expected CMSSM Higgs production cross sections and decay branching ratios $\sigma \times \mathcal{B}$ normalized by the corresponding values expected for those of a SM Higgs boson of the same mass. The results are compared with the precisions expected at each collider, and allow for a direct comparison of the different channels. The measurements in the Higgs sector are found to provide important consistency tests of the CMSSM. We then generalize our analysis to the case of a non-universal Higgs model (NUHM), where the values of $M_A$ and $\mu$ are independent parameters. We explore in particular the sensitivity to $M_A$, finding that measurements at $e^+e^-$, $\gamma\gamma$ and $\mu^+\mu^-$ colliders could yield indirect constraints on its value, up to $M_A \sim 1200$ GeV. We discuss the potential of these measurements for distinguishing between the CMSSM and the NUHM, probing in this way the assumption of universality.

# 1 Introduction

In a previous paper [1], we discussed the observability at the Tevatron and the LHC of the lightest neutral Higgs boson in the constrained MSSM (CMSSM) [1], in which the soft supersymmetry-breaking parameters are assumed to be universal at some high GUT input scale [2]. Our conclusions were in general quite encouraging, in the sense that the products of hadronic production cross sections and branching ratios $\sigma \times \mathcal{B}$ in the CMSSM differ little from those in the Standard Model (SM), so that a CMSSM Higgs boson should be essentially as observable at the Tevatron or the LHC as would be a SM Higgs boson with the same mass.

On the other hand, the expected precision in measuring the Higgs boson properties was found to be too small to establish deviations in the properties of the lightest CMSSM Higgs boson from a SM Higgs boson with the same mass. As an example, the decay $h \to \gamma\gamma$, which is the prime discovery channel for a CMSSM or SM Higgs boson weighing $\sim 120$ GeV, has been analyzed in [1]. The statistical error is expected to be $\sim 1$ % and the parton-parton luminosity error about 5 %. If the theoretical error in the calculation of the parton-parton cross section could be neglected, there could be a 2-$\sigma$ difference between the strengths of the CMSSM and SM signals. However, this may well be masked by the theoretical error in the cross-section calculation, which is currently $\gtrsim 20$ % [3], so the LHC may not be able to discriminate between CMSSM and SM Higgs bosons. Thus the onus may fall on a subsequent lepton collider to discriminate between them.

If supersymmetry as a low-energy theory is realized in nature, it is likely that supersymmetric particles will be detected at the LHC and future lepton colliders [4]. While the observation of supersymmetric particles would of course rule out the SM, it would nevertheless be crucial to establish also that the Higgs sector has the properties predicted within the MSSM. This holds in particular if only one light Higgs boson which resembles the SM one is observed at the LHC. A direct measurement of the heavy Higgs boson states of the MSSM might be difficult or impossible, depending on $\tan\beta$. For example, at the LHC there is a wedge in the $(M_A, \tan\beta)$ plane where the heavy Higgs bosons cannot be detected, and direct observability at a lepton collider is limited by the available centre-of-mass energy: see, e.g., [5]. Even in the case where additional Higgs bosons are observed, the precise measurements of the properties of the lightest $\mathcal{CP}$-even Higgs boson will provide important consistency tests of the model.

In this paper, we consider and compare the prospects of $e^+e^-$ (LC), $\gamma\gamma$ ($\gamma$C) and $\mu^+\mu^-$ ($\mu$C) colliders for establishing the supersymmetric nature of the lightest $\mathcal{CP}$-even Higgs boson, as compared to the properties a SM Higgs boson of the same mass would have. We consider the principal Higgs observation channels at each collider, see Table 1, including their respective anticipated accuracies [6–10]. In each case, we calculate the strength expected for

[1] For a comparison of the Higgs-sector properties of the CMSSM with gauge- and anomaly-mediated (GMSB and AMSB) scenarios, see [2].

[2] An economical way to ensure this universality is by gravity-mediated supersymmetry breaking in a minimal supergravity (mSUGRA) scenario, but there are other ways to validate the CMSSM assumptions, including no-scale supergravity scenarios.

| collider | production mode | decay mode | precision |
|---|---|---|---|
| LC | $e^+e^- \to Z^* \to Zh$ | $h \to b\bar{b}$ | 1.5% |
| LC | | $h \to \tau^+\tau^-$ | 4.5% |
| LC | | $h \to c\bar{c}$ | 6% |
| LC | | $h \to gg$ | 4% |
| LC | | $h \to WW^*$ | 3% |
| $\gamma$C | $\gamma\gamma \to h$ | $h \to b\bar{b}$ | 2% |
| $\gamma$C | | $h \to WW^*$ | 5% |
| $\gamma$C | | $h \to \gamma\gamma$ | 11% |
| $\mu$C | $\mu^+\mu^- \to h$ | $h \to b\bar{b}$ | 3% |

Table 1: *Expected precisions in the measurements of Higgs observables at the LC, the $\gamma$C and the $\mu$C for the light $\mathcal{CP}$-even Higgs boson of the MSSM. The production mode of the LC refers to running at energies of $\sqrt{s} = 350$–$500$ GeV.*

a CMSSM Higgs signal normalized relative to the SM signal

$$\frac{\left[\sigma \times \mathcal{B}\right]_{\rm CMSSM}}{\left[\sigma \times \mathcal{B}\right]_{\rm SM}}, \tag{1}$$

as evaluated in [11,12]. We display our results in planes of the universal soft supersymmetry-breaking gaugino mass $m_{1/2}$ and scalar mass $m_0$, for different representative values of $\tan\beta$, the trilinear soft supersymmetry-breaking parameter $A_0$ and the sign of the supersymmetric Higgs parameter $\mu$. In each case, we restrict our attention to the regions of parameter space still permitted by the direct search limits on sparticle [13] and Higgs masses [14], the indirect constraints from $b \to s\gamma$ [15, 16], $g_\mu - 2$ [17], and the cosmological relic density $\Omega_\chi h^2$ [18], which we require to lie between 0.1 and 0.3 [19]. In this way, we identify the regions of the CMSSM parameter space in which a certain channel may distinguish between CMSSM and SM Higgs bosons with the same mass.

The mass of the $\mathcal{CP}$-odd Higgs boson, $M_A$, plays a key role in the investigation of any MSSM scenario. Since, as discussed above, the direct measurement of $M_A$ might be very difficult, it will be very important to obtain indirect information about this parameter that can be confronted with the predictions of the CMSSM or other supersymmetry-breaking scenarios. Specifically, we analyze a scenario in which the assumption made in the CMSSM of universality between the soft supersymmetry-breaking masses of the Higgs multiplets and those of the squarks and sleptons is relaxed, a framework we term the non-universal Higgs model (NUHM) [20]. Such non-universality releases $\mu$ and $M_A$ from the values that are fixed for them in the CMSSM, while otherwise the spectrum of the supersymmetric particles resembles the one in the CMSSM. Since in the decoupling limit, $M_A \gg M_Z$, the Higgs sector

of the MSSM becomes SM-like, deviations in the production and decay of the lightest $\mathcal{CP}$-even Higgs boson of the MSSM from the SM values can be translated into an upper bound on $M_A$. Therefore, we seek in this paper to identify the regions of the MSSM parameter space in which an indirect limit on $M_A$ can be obtained from $h$ measurements alone, even if the $A$ boson cannot be observed directly.

The sensitivity of the Higgs sector observables to variations in $M_A$ allows one to test the universality assumption of the CMSSM. Precise determinations of $\sigma \times \mathcal{B}$ can in this way be used to distinguish between the CMSSM and the NUHM. We investigate the potential of the different colliders for setting limits on the deviations of $\mu$ and $M_A$ from their CMSSM values.

The rest of the paper is organized as follows. In Sect. 2, we summarize the CMSSM parameter space and its phenomenological constraints. In Sect. 3, we discuss in which channel the lightest CMSSM Higgs boson can best be distinguished from a SM Higgs boson with the same mass, at various accelerators. The indirect reach in $M_A$ and possible tests of the CMSSM universality assumption are discussed in Sect. 4 Our conclusions are presented in Sect. 5.

# 2 Phenomenological Constraints

Before describing our results in detail, we first review our treatment of the experimental and cosmological constraints on the CMSSM parameter space.

Our treatment of the direct LEP constraints on sparticle masses is described in [1], so we do not describe it further here. The LEP Higgs constraint within the SM is now $m_H > 114.4$ GeV, while the data show a 1.7-$\sigma$ excess over the background expectation compatible with a Higgs signal with mass $\sim 116$ GeV [14]. As pointed out previously, the $ZZh$ coupling in the CMSSM is very close to that of the SM Higgs for almost all possible parameter values (see [2], however), so the SM Higgs boson mass limit can be carried over to the CMSSM for most of the parameter space. In this paper, we allow only CMSSM parameter choices that are consistent with $m_h > 113$ GeV as calculated for $m_t = 175$ GeV using the `FeynHiggs` code [21, 22] in its latest implementation [23], which includes various recent results [24–26]. We have chosen a somewhat weaker limit than the actual SM exclusion bound, owing to remaining theoretical uncertainties from unknown higher-order corrections [23]. The measured value of $m_h$, which experimentally will be known with high precision in this scenario, will provide very valuable consistency tests of the model, provided that the theoretical uncertainties in the $m_h$ prediction can be reduced below the level of about 1 GeV. Thus, besides the bound $m_h > 113$ GeV, for reference we also include in our plots the contours $m_h = 115, 117, 120, 125$ GeV. In view of the experimental bounds on $m_h$, we do not consider values of $\tan\beta$ below 10, since in the CMSSM the low-$\tan\beta$ region is severely constrained by the experimental bound on the Higgs-boson mass.

In our treatment of $b \to s\gamma$, we follow [1, 27] in our implementation of NLO QCD corrections at large $\tan\beta$ [16]. We assume the 95% confidence-level range $2.33 \times 10^{-4} < \mathcal{B}(b \to s\gamma) < 4.15 \times 10^{-4}$ [15], and we accept all CMSSM parameter sets that give predictions in this range, allowing for the scale and model dependences of the QCD calculations.

The situation with regard to $a_\mu \equiv (g_\mu - 2)/2$ has changed significantly since [1]. Concerning the theory evaluation, the light-by-light contribution has been corrected [28]. Concerning

the experimental precision, a new result has recently been released by the E821 collaboration, including the year 2000 data [17], which lead to a reduction in the experimental error by roughly a factor of 2. The magnitude of the deviation from the SM result is now at $\delta a_\mu = (33.9 \pm 11.2) \times 10^{-10}$ [29] using $e^+e^-$ data for the hadronic vacuum polarization contribution in the SM prediction, and by $\delta a_\mu = (16.7 \pm 10.7) \times 10^{-10}$ [29] based on $\tau$ decay data. Other recent analyses of the $e^+e^-$ data yield similar results [30]. We take the 2-$\sigma$ range to be $11.5 \times 10^{-10} < \delta a_\mu < 56.3 \times 10^{-10}$. This means that $\mu < 0$ is no longer allowed. In the following plots, we display as solid, thick, red diagonal lines the $\pm$2-$\sigma$ contours in the $(m_{1/2}, m_0)$ plane. However, we also show as thin red lines the results of the more conservative theoretical estimate (based on the $\tau$ data) $-4.7 \times 10^{-10} < \delta a_\mu < 38.1 \times 10^{-10}$, which allows some regions of parameter space with $\mu < 0$.

As in [1], we assume $R$-parity conservation, so that the lightest supersymmetric particle (LSP), presumed to be the lightest neutralino $\chi$, is stable and may have an interesting cosmological relic density $\Omega_\chi h^2$. We accept CMSSM parameter sets that have $0.1 \leq \Omega_\chi h^2 \leq 0.3$ as calculated using the code documented in [4,27]. Lower values of $\Omega_\chi h^2$ would be allowed if not all the cosmological dark matter is composed of neutralinos. However, larger values of $\Omega_\chi h^2$ are excluded by cosmology, and even values as large as 0.3 are disfavoured by the most recent global fits to cosmological data [19,31].

# 3 Sensitivity of Higgs-sector observables to deviations of the CMSSM from the SM

In this Section we complete the survey of Higgs production and decay channels, which we started for hadron colliders in [1]. Here we present analogous results for the LC, the $\gamma$C and the $\mu$C for the channels given in Table 1. We present our results in $(m_{1/2}, m_0)$ planes for $\tan\beta = 10$, $\mu > 0$ and $A_0 = 0$, for $\tan\beta = 50$, $\mu > 0$ and $A_0 = 0$ or $-2m_{1/2}$, and for $\tan\beta = 35$, $\mu < 0$ and $A_0 = m_{1/2}$. The irregularities in the cosmological region in panel (a) etc., and the separations between the dots in panel (b) etc. are due to the finite grid size used in our sampling of parameter space. The figures are provided with $M_A$ contours, showing the sensitivity of each channel to this fundamental parameter of the Higgs boson sector. The resultant indirect constraints on $M_A$ are discussed in Section 4.

## 3.1 Observables at an $e^-e^+$ Linear Collider

Fig. 1 shows our results for $\sigma(e^+e^- \to Zh) \times \mathcal{B}(h \to b\bar{b})$ in the $(m_{1/2}, m_0)$ plane. We have chosen the same representative set of parameters for this and the products $\sigma \times \mathcal{B}$ for all the other channels. The upper left (right) plot shows the results for $\tan\beta = 10(50)$, $A_0 = 0$ and $\mu > 0$. The lower left plot shows $\tan\beta = 35$, $A_0 = m_{1/2}$ and $\mu < 0$, and the lower right plot is for $\tan\beta = 50$, $A_0 = -2m_{1/2}$ and $\mu > 0$. We only show one plot for each channel for $\mu < 0$, since this sign of $\mu$ is disfavored by the recent $g_\mu - 2$ measurement [17] as well as by the $\mathcal{B}(b \to s\gamma)$ constraint [15,16]. The thick solid diagonal red lines show the $\pm 2-\sigma$ range of $g_\mu - 2$ for the standard value of the discrepancy $\delta a_\mu = (33.9 \pm 11.2) \times 10^{-10}$, and the thin red lines correspond to the more conservative estimate $\delta a_\mu = (16.7 \pm 10.7) \times 10^{-10}$. For $\mu > 0$, we have $2-\sigma$ lower bounds on $(m_{1/2}, m_0)$ from both theory evaluations, while only the standard estimate also results in upper bounds. The more conservative estimate also yields a thin red

line for $\mu < 0$, where the parameter space to the left is excluded experimentally. The nearly vertical solid (dotted, short-dashed, dot-dashed and long-dashed) black lines correspond to the contours [21] $m_h = 113$ $(115, 117, 120, 125)$ GeV, where the latter one is only visible in the scenario with $\mu < 0$ for large values of $m_{1/2}$. The regions excluded by $\mathcal{B}(b \to s\gamma)$ are shown as the pink shaded areas, that are more prominent in the $\mu < 0$ case [3]. Finally, the large bricked region in the lower right part of each plot corresponds to the region in which the lightest $\tilde{\tau}$ is the LSP, which is excluded because the LSP cannot be charged. The colored area is that where the relic density of the neutralino LSP is in the range $0.1 < \Omega_\chi h^2 < 0.3$ preferred by cosmology.

In Fig. 1 and subsequent figures, we code with different shadings domains of the CMSSM parameter space, consistent with the direct and cosmological constraints mentioned above, where the CMSSM prediction differs from the SM by different numbers of standard deviations $\sigma$, as estimated on the basis of the precisions quoted in Table 1.

We see in Fig. 1 that the channel $\sigma(e^+e^- \to Zh) \times \mathcal{B}(h \to b\bar{b})$ exhibits large deviations from the SM only for $\mu < 0$ and $m_{1/2} < 1000$ GeV, a region that is excluded by $\mathcal{B}(b \to s\gamma)$ and disfavoured by $g_\mu - 2$. For $\mu > 0$, deviations of 2 or 3 $\sigma$ are only observed for $\tan\beta = 10$ with very low $m_{1/2}$, otherwise the deviations are below the $2-\sigma$ level. This means that, on the one hand, the LC will have no problem in observing the lightest CMSSM Higgs boson in this channel. On the other hand, it will not be easy to obtain additional indirect information on the CMSSM Higgs sector by the precise measurement of this channel; see, however, Sect. 4.

The interplay between the measurement of $\sigma \times \mathcal{B}$ and the measurement of the Higgs-boson mass can be seen from the contour lines indicating different values of $m_h$. The compatibility of the $m_h$ measurement with the results for $\sigma \times \mathcal{B}$ (and with possible information on the sparticle spectrum) is a stringent consistency test of the CMSSM. For instance, a measurement of $m_h \gtrsim 118$ GeV in Fig. 1a (upper left panel) would be compatible only with values of $\sigma(e^+e^- \to Zh) \times \mathcal{B}(h \to b\bar{b})$ that differ from the SM value by not more than one standard deviation. Observation of a significantly larger deviation of $\sigma(e^+e^- \to Zh) \times \mathcal{B}(h \to b\bar{b})$ from the SM value with $m_h \approx 118$ GeV would disfavor an interpretation within the CMSSM for the parameters of Fig. 1a.

The results in the $\sigma(e^+e^- \to Zh) \times \mathcal{B}(h \to \tau^+\tau^-)$ channel, which are not shown here, are similar in pattern to the $\sigma(e^+e^- \to Zh) \times \mathcal{B}(h \to b\bar{b})$ channel. The deviations from the SM, however, are somewhat smaller in the $h \to \tau^+\tau^-$ case.

Fig. 2 shows the channel $\sigma(e^+e^- \to Zh) \times \mathcal{B}(h \to c\bar{c})$. Here the situation is different from that in the $h \to b\bar{b}$ decay channel, as the CMSSM result is always somewhat smaller than the corresponding SM result. This is due to the enlarged value of $\mathcal{B}(h \to b\bar{b})$, see Fig. 1, which reduces the branching ratio for the $h \to c\bar{c}$ mode. The absolute sizes of the deviations are similar to those in the $h \to b\bar{b}$ case. As before, the largest deviations again occur for negative $\mu$ in the experimentally excluded part of the parameter space. The largest deviations in the allowed part of parameter space are for $\tan\beta = 10$ and small $m_{1/2}$, where 2- to 3-$\sigma$ deviations may be attained.

The LC survey is completed by Fig. 3, in which the $\sigma(e^+e^- \to Zh) \times \mathcal{B}(h \to WW^*)$ channel is shown. Here the CMSSM signal is always smaller than the corresponding SM result, with the enhancement of $\mathcal{B}(h \to b\bar{b})$ again playing a role. In addition, the decay

[3] In Fig. 1a, where the $b \to s\gamma$ bound yields much weaker constraints than the search limits on $m_h$ and the supersymmetric particles, the region excluded by $b \to s\gamma$ is not shown.

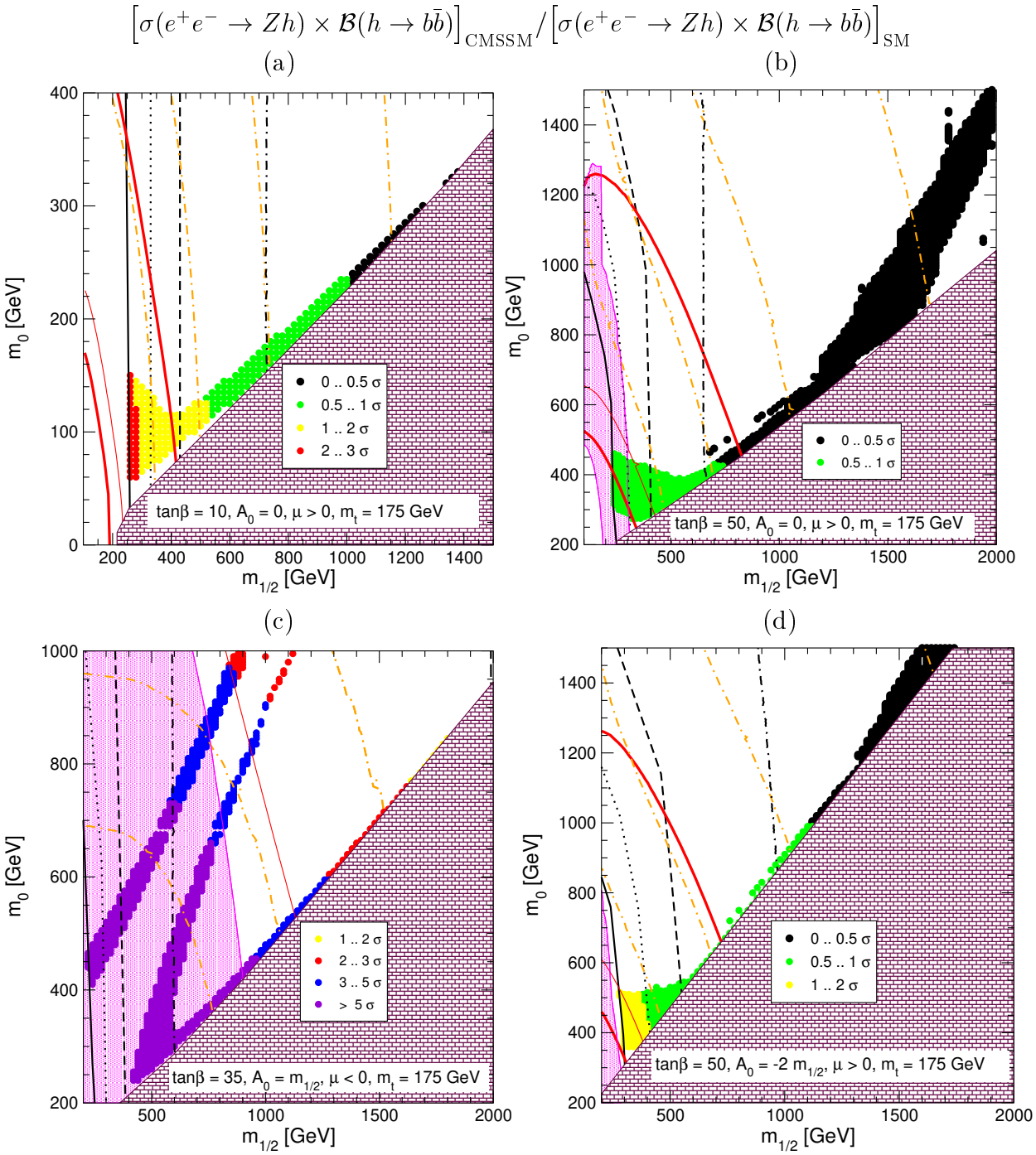


Figure 1: *The deviations of* $\sigma(e^+e^- \to Zh) \times \mathcal{B}(h \to b\bar{b})$ *for the lightest* $\mathcal{CP}$*-even CMSSM Higgs boson, normalized to the value in the SM with the same Higgs mass, are given in the* $(m_{1/2}, m_0)$ *planes for* $\mu > 0$, $\tan\beta = 10, 50$ *and* $A_0 = 0$ *(upper row), for* $\mu > 0$, $\tan\beta = 50$ *and* $A_0 = -2m_{1/2}$ *(lower right) and for* $\mu < 0$, $\tan\beta = 35$ *and* $A_0 = m_{1/2}$ *(lower left). In all plots* $m_t = 175$ GeV *has been used. The diagonal red thick (thin) lines are the* $\pm 2 - \sigma$ *contours for* $g_\mu - 2$*: +56.3, +11.5 (+38.1, -4.7). The near-vertical solid, dotted short-dashed, dash-dotted and long-dashed (black) lines are the* $m_h = 113, 115, 117, 120, 125$ GeV *contours. The lighter dot-dashed (orange) lines correspond to* $M_A = 500, 700, 1000, 1500$ GeV*. The light shaded (pink) regions are excluded by* $b \to s\gamma$*. The (brown) bricked regions are excluded because the LSP is the charged* $\tilde{\tau}_1$ *in these regions.*

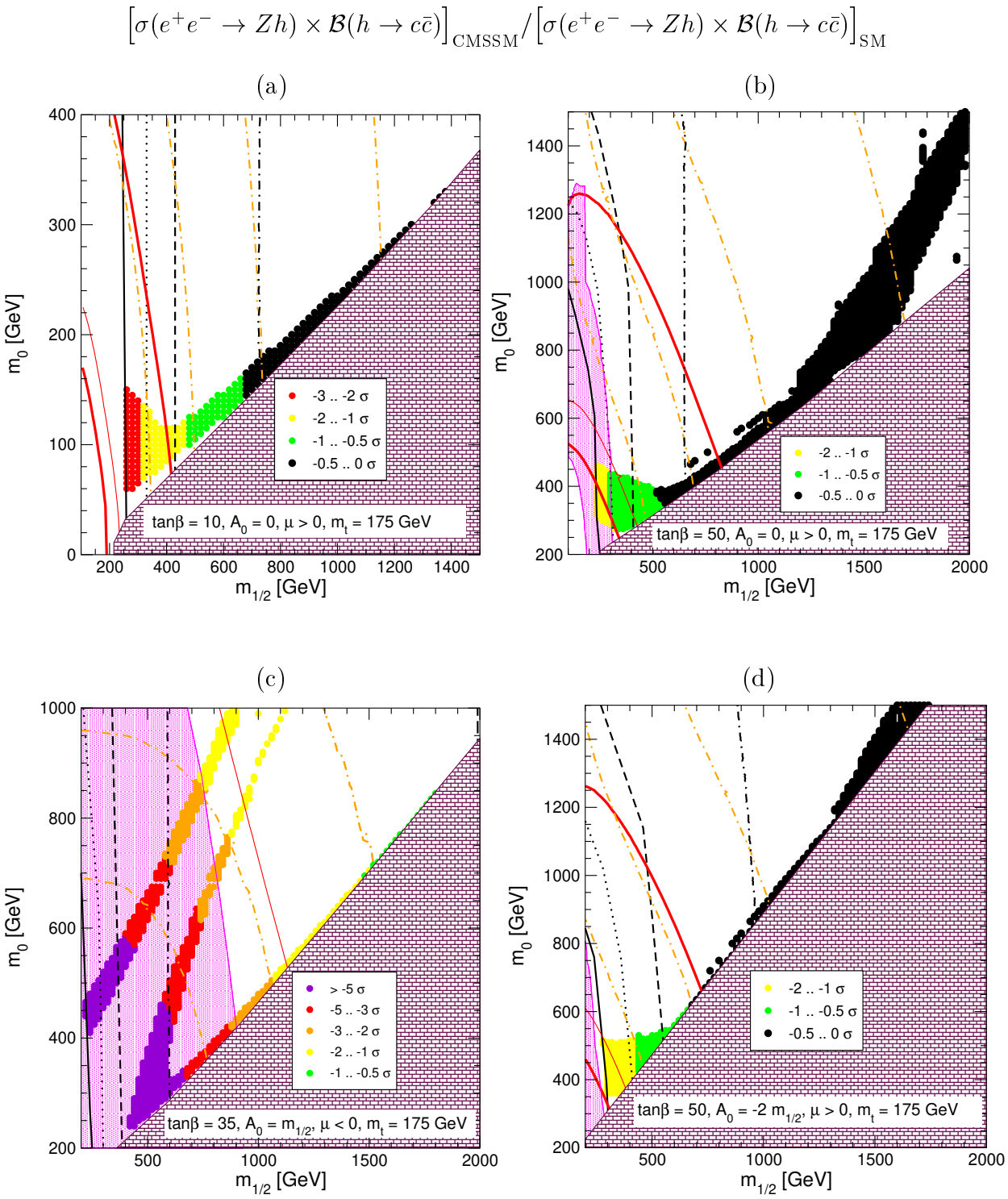


Figure 2: *The deviations of* $\sigma(e^+e^- \to Zh) \times \mathcal{B}(h \to c\bar{c})$ *for the lightest* $\mathcal{CP}$*-even CMSSM Higgs boson, normalized to the value for a SM Higgs boson with the same mass, are given in the* $(m_{1/2}, m_0)$ *planes for* $\mu > 0$, $\tan\beta = 10, 50$ *and* $A_0 = 0$ *(upper row), for* $\mu > 0$, $\tan\beta = 50$ *and* $A_0 = -2m_{1/2}$ *(lower right) and for* $\mu < 0$, $\tan\beta = 35$ *and* $A_0 = m_{1/2}$ *(lower left). In all plots* $m_t = 175$ GeV *has been used. The contours and shadings are the same as in Fig. 1.*

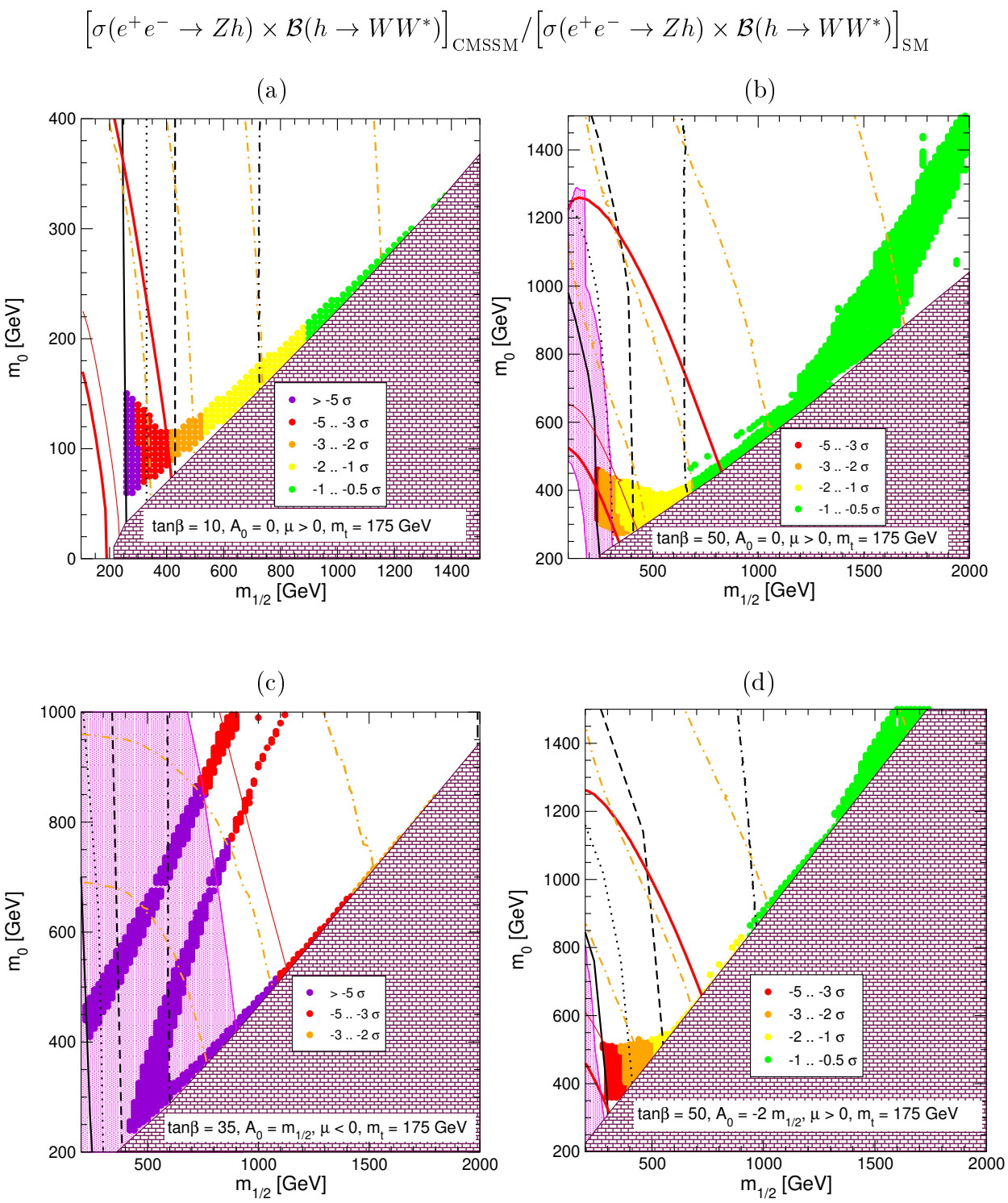


Figure 3: *The deviations of* $\sigma(e^+e^- \to Zh) \times \mathcal{B}(h \to WW^*)$ *for the lightest* $\mathcal{CP}$*-even CMSSM Higgs boson, normalized to the value for a SM Higgs boson with the same mass, are given in the* $(m_{1/2}, m_0)$ *planes for* $\mu > 0$, $\tan\beta = 10, 50$ *and* $A_0 = 0$ *(upper row), for* $\mu > 0$, $\tan\beta = 50$ *and* $A_0 = -2m_{1/2}$ *(lower right) and for* $\mu < 0$, $\tan\beta = 35$ *and* $A_0 = m_{1/2}$ *(lower left). In all plots* $m_t = 175$ GeV *has been used. The contours and shadings are the same as in Fig. 1.*

$h \to WW^*$ is always suppressed in the MSSM, because of the additional coupling factor $\sin^2(\beta-\alpha) \lesssim 1$, though this suppression has only a marginal effect in the CMSSM parameter space. The largest deviations again occur for $\mu < 0$, but deviations of $5\sigma$ or more can be observed also for $\mu > 0$. While such a suppression should not endanger the observability of this channel, the sizable deviations from the SM prediction provide a sensitive consistency test of the CMSSM and allow one to obtain valuable indirect information on the Higgs boson sector, as shown in more detail in Sect. 4.

### 3.2 Observables at a $\gamma\gamma$ Collider

We now turn to the channels accessible at a $\gamma$C, which might become available some time after the construction of a LC. In Fig. 4 we first show results for the main Higgs decay channel, $\sigma(\gamma\gamma \to h) \times \mathcal{B}(h \to b\bar{b})$. This looks quite similar to the corresponding LC results, and the same is true for the $\sigma(\gamma\gamma \to h) \times \mathcal{B}(h \to WW^*)$ channel, which is not shown here.

We show in Fig. 5 results for the additional observable at the $\gamma$C, namely $\sigma(\gamma\gamma \to h) \times \mathcal{B}(h \to \gamma\gamma)$. This channel can be isolated from the background using the feature that the signal, contrary to the background, peaks sharply in the forward region [8, 9]. However, the precision expected is only at the 11% level, so that no large deviations will be observable. As seen in Fig. 5, for $\mu > 0$ they always stay below the $2-\sigma$ level, and only in the excluded region with $\mu < 0$ do larger deviations occur.

### 3.3 Observables at a $\mu^+\mu^-$ Collider

This survey is completed with the main channel at the $\mu$C, namely the channel $\sigma(\mu^+\mu^- \to h) \times \mathcal{B}(h \to b\bar{b})$ shown in Fig. 6. Due to the similar coupling structures in the Higgs production channel, $\mu^+\mu^- \to h$, and in the Higgs decay channel, $h \to b\bar{b}$, the deviations can be relatively large, potentially exceeding $5\sigma$ even for positive $\mu$. Therefore, in principle, it should be possible to extract more indirect information about the CMSSM Higgs boson sector. However, we expect that any $\mu$C will come into operation only after the other colliders considered above. Thus, a large variety of direct and indirect results should already be available when the $\mu$C starts running, making it rather difficult to speculate about the impact of the prospective $\mu$C precision measurements. The $\mu$C has in particular the potential for measuring $m_h$ with a spectacular precision [10], which however needs to be confronted with the parametric and higher-order uncertainties in the Higgs-mass prediction. For investigating the MSSM Higgs sector, a higher-energy $\mu$C capable of producing directly the $\mathcal{CP}$-odd and -even CMSSM Higgs bosons $A, H$ might also become an interesting option, but studying the potential of such a machine lies beyond the scope of this paper.

## 4 Testing the CMSSM Universality Assumption and Indirect Constraints on $M_A$

The MSSM Higgs sector can be characterized at lowest order by the values of $\tan\beta$ and the mass of the $\mathcal{CP}$-odd Higgs boson, $M_A$. As already mentioned, at the LHC there is a substantial part of parameter space where the heavy Higgs bosons cannot be observed, the so-called 'wedge region' [32, 33]. On the other hand, $M_A$ might well be too large for direct

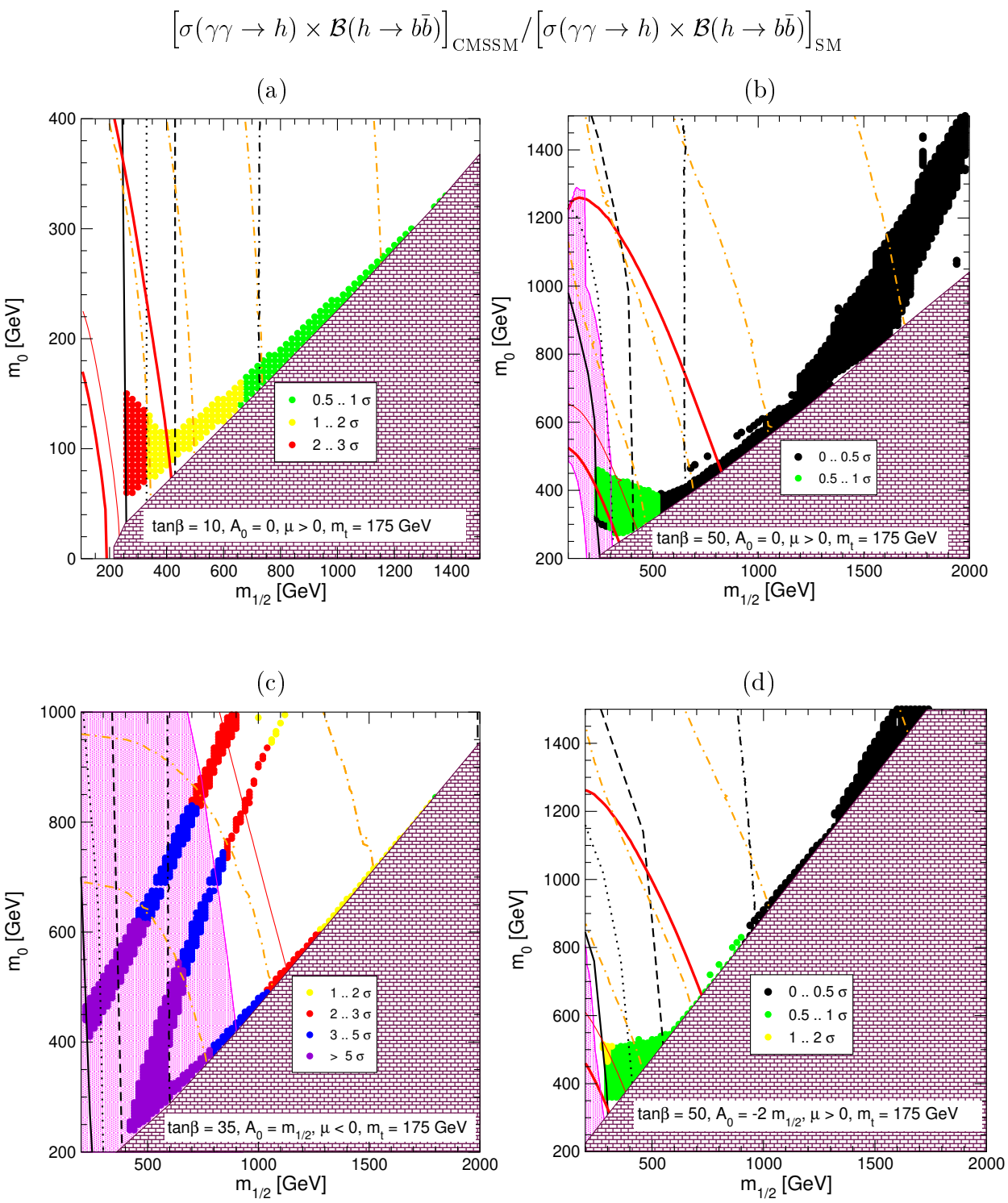


Figure 4: *The deviations of* $\sigma(\gamma\gamma \to h) \times \mathcal{B}(h \to b\bar{b})$ *for the lightest* $\mathcal{CP}$*-even CMSSM Higgs boson, normalized to the value in the SM with the same Higgs mass, are given in the* $(m_{1/2}, m_0)$ *planes for* $\mu > 0$, $\tan\beta = 10, 50$ *and* $A_0 = 0$ *(upper row), for* $\mu > 0$, $\tan\beta = 50$ *and* $A_0 = -2m_{1/2}$ *(lower right) and for* $\mu < 0$, $\tan\beta = 35$ *and* $A_0 = m_{1/2}$ *(lower left). The contours and shadings are the same as in Fig. 1.*

$$\left[\sigma(\gamma\gamma \to h) \times \mathcal{B}(h \to \gamma\gamma)\right]_{\rm CMSSM} / \left[\sigma(\gamma\gamma \to h) \times \mathcal{B}(h \to \gamma\gamma)\right]_{\rm SM}$$

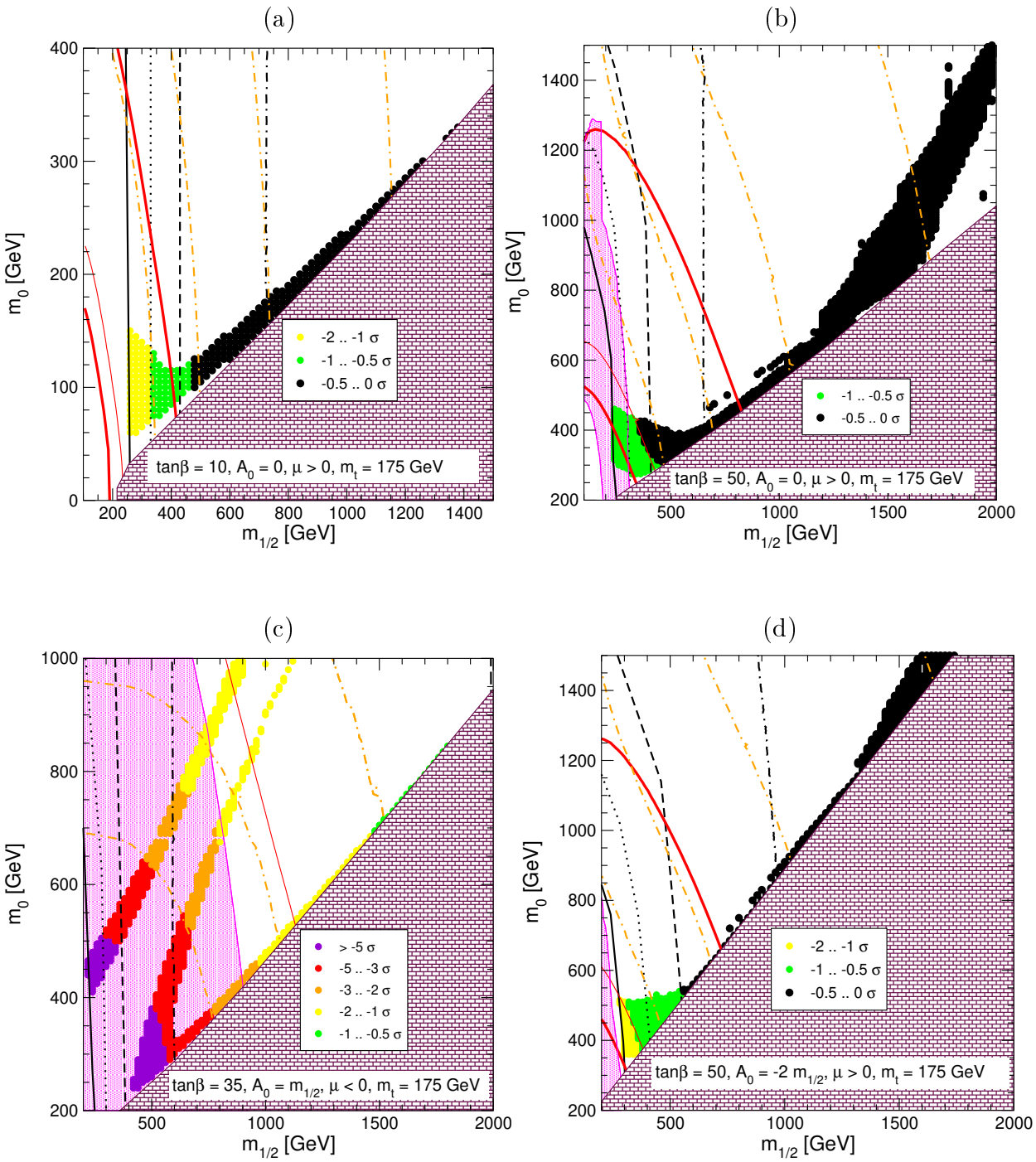


Figure 5: *The deviations of* $\sigma(\gamma\gamma \to h) \times \mathcal{B}(h \to \gamma\gamma)$ *for the lightest* $\mathcal{CP}$*-even CMSSM Higgs boson, normalized to the value for a SM Higgs boson with the mass, are given in the* $(m_{1/2}, m_0)$ *planes for* $\mu > 0$, $\tan\beta = 10, 50$ *and* $A_0 = 0$ *(upper row), for* $\mu > 0$, $\tan\beta = 50$ *and* $A_0 = -2m_{1/2}$ *(lower right) and for* $\mu < 0$, $\tan\beta = 35$ *and* $A_0 = m_{1/2}$ *(lower left). In all plots* $m_t = 175$ GeV *has been used. The contours and shadings are the same as in Fig. 1.*

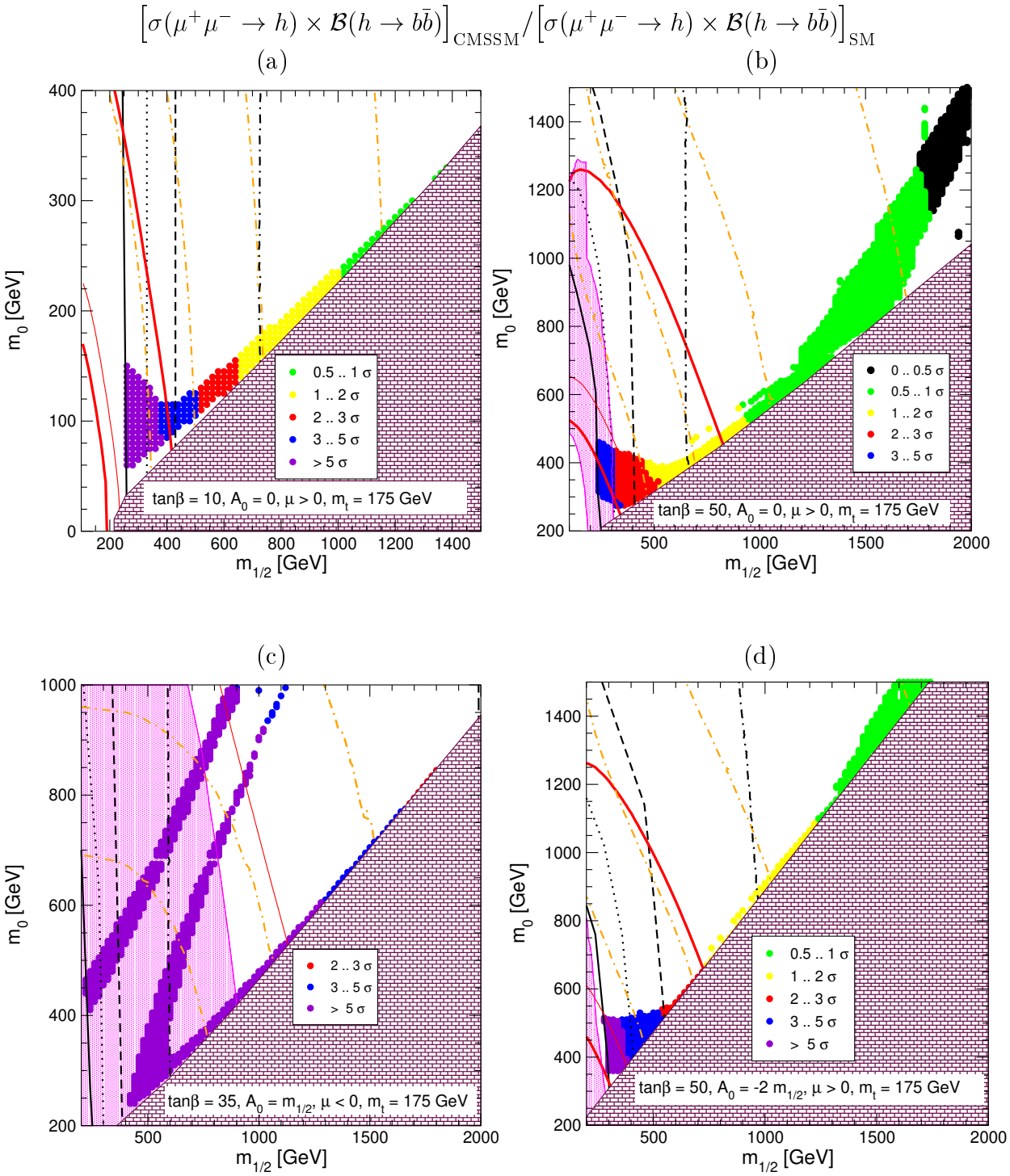


Figure 6: *The deviations of* $\sigma(\mu^+\mu^- \to h) \times \mathcal{B}(h \to b\bar{b})$ *for the lightest* $\mathcal{CP}$*-even CMSSM Higgs boson, normalized to the value in the SM with the same Higgs mass, are given in the* $(m_{1/2}, m_0)$ *planes for* $\mu > 0$, $\tan\beta = 10, 50$ *and* $A_0 = 0$ *(upper row), for* $\mu > 0$, $\tan\beta = 50$ *and* $A_0 = -2m_{1/2}$ *(lower right) and for* $\mu < 0$, $\tan\beta = 35$ *and* $A_0 = m_{1/2}$ *(lower left). In all plots* $m_t = 175$ GeV *has been used. The contours and shadings are the same as in Fig. 1.*

observation at the LC: $M_A \gtrsim \sqrt{s}/2$. In this case one would have to rely on indirect methods to constrain the possible values of $M_A$. Exploratory studies in some (favorable) scenarios can be found in [11, 34], also including information from GigaZ [35].

In the CMSSM, $M_A$ is fixed by the electroweak vacuum conditions in terms of $\tan\beta$, $m_{1/2}$, $m_0$ and $A_0$. However, in a more general scenario like a non-universal Higgs model (NUHM) [20, 36] the CMSSM assumption that the soft supersymmetry-breaking masses for the Higgs multiplets are the same as those for squarks and sleptons may be relaxed. In this case the values of $M_A$ and $\mu$ become independent parameters, though their ranges are restricted by various theoretical and phenomenological constraints. Accordingly, even if experimental results on the spectrum of supersymmetric particles turn out to be compatible with the predictions of the CMSSM scenario, confronting the CMSSM prediction for $M_A$ with direct or indirect information on this parameter provides a non-trivial test of the model.

In the decoupling limit, $M_A \gg M_Z$, the couplings of the light $\mathcal{CP}$-even Higgs boson of the MSSM become equal to those of the SM Higgs boson. Thus, the observation of deviations in the production and decay of the lightest $\mathcal{CP}$-even Higgs boson of the MSSM from the SM values would allow one to set an upper (or lower) limit on the mass of $M_A$.

In order to facilitate the analysis of indirect sensitivities to $M_A$ at different colliders in this context, we have also shown in Fig. 1 - 6 the contour lines for $M_A = 500, 700, 1000, 1500$ GeV, as light (orange) dot-dashed lines from left to right. Sometimes the 1500 GeV line is missing; it would appear at larger $m_{1/2}$. For given values of $A_0$, $\tan\beta$ and the sign of $\mu$, these contour lines indicate that a measurement of $\sigma \times \mathcal{B}$ in a certain channel translates into an allowed interval of $M_A$ values.

The contour lines indicating different values of $M_A$ within the CMSSM can also be interpreted within the NUHM. For the same values of the parameters $m_0$, $m_{1/2}$, $A_0$, $\tan\beta$ and $\mu$ in the NUHM as in the CMSSM (see below for a discussion of the $\mu$-dependence in the NUHM), decreasing the value of $M_A$ within the NUHM compared to the value in the CMSSM will increase the deviation of $\sigma \times \mathcal{B}$ from the SM prediction and vice versa. In this way measurements of $\sigma \times \mathcal{B}$ can be used to establish an upper bound on $M_A$ within the NUHM.

We first focus on the LC. For $\tan\beta = 10$, the channel $\sigma(e^+e^- \to Zh) \times \mathcal{B}(h \to WW^*)$ offers the best prospects. An observation of a deviation of more than 3 (2, 1) $\sigma$ can be interpreted as an upper limit on $M_A$ of $\sim 600$ $(750, 1200)$ GeV. We note that the decays $h \to b\bar{b}$ and $h \to c\bar{c}$ also show some sensitivity for this parameter set. However, the situation is somewhat worse when $\tan\beta = 50$. For large and negative $A_0 = -2m_{1/2}$, limits of $M_A \lesssim 550, 900$ GeV can be set at the $2-, 1-\sigma$ level, but the sensitivity decreases with increasing $A_0$. In particular, for $A_0 = +m_{1/2}$ only very small deviations from the SM predictions occur, and there is hardly any capability of setting an upper bound on $M_A$.

Our results are shown in more detail in Fig. 7. The deviations of the CMSSM predictions for $\sigma(e^+e^- \to Zh) \times \mathcal{B}(h \to b\bar{b})$ (upper row) and $\sigma(e^+e^- \to Zh) \times \mathcal{B}(h \to WW^*)$ (lower row) from the SM values are shown now in the $(M_A, m_0)$ plane. For given values of $A_0$, $\tan\beta$ and the sign of $\mu$, the allowed interval for $M_A$ in the CMSSM compatible with a certain deviation of $\sigma \times \mathcal{B}$ from the SM value can be read off directly. If one also has information on $m_0$ and $m_{1/2}$, this can be compared with the value predicted for $M_A$ within the CMSSM.

Within the NUHM, the indirect constraints on $M_A$ obtained from the Higgs sector observables are analogous to the constraints on the SM Higgs from the electroweak precision data. A direct measurement of the value of $M_A$ itself will provide a thorough consistency

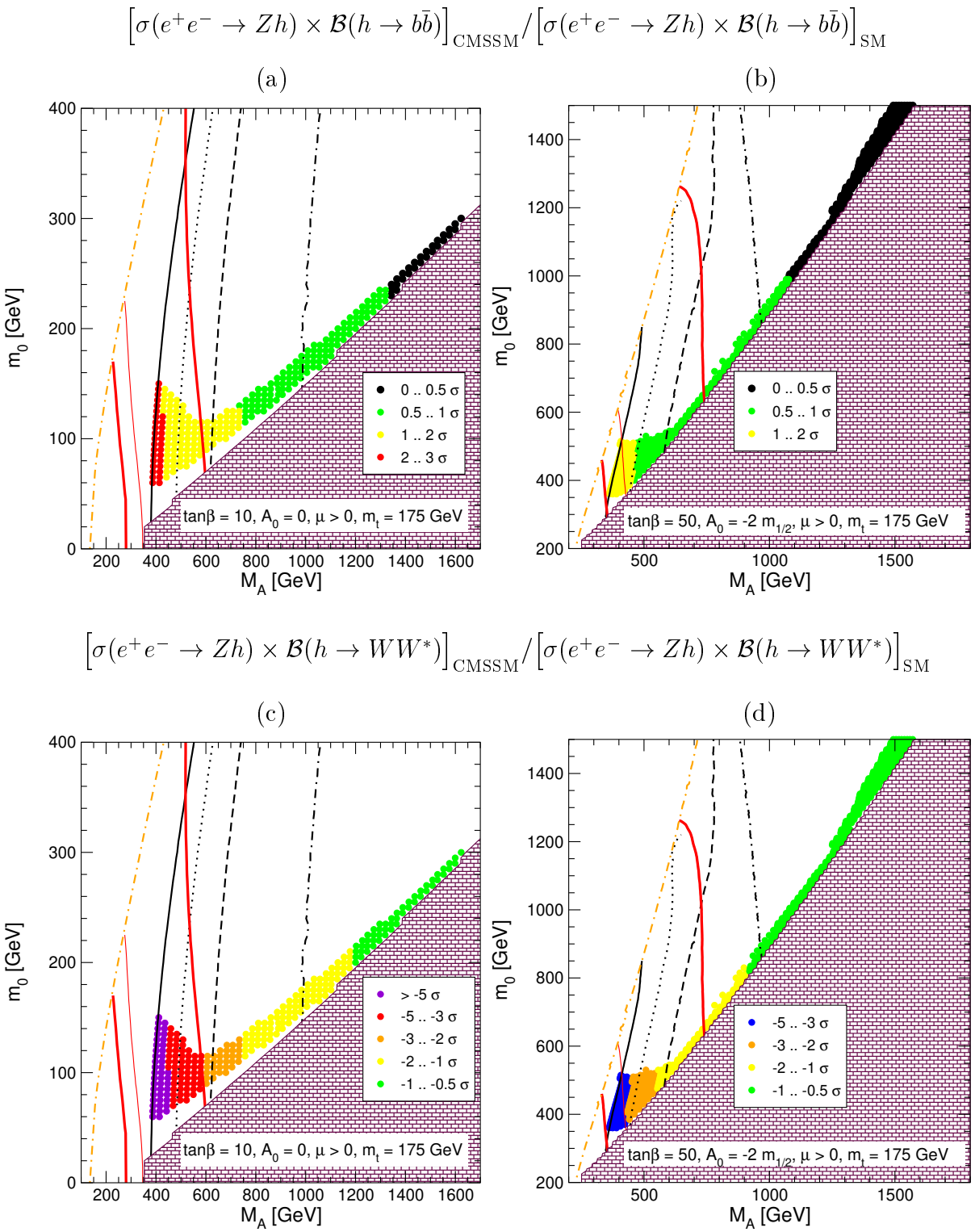


Figure 7: *The deviations of* $\sigma(e^+e^- \to Zh) \times \mathcal{B}(h \to b\bar{b})$ *(upper row) and* $\sigma(e^+e^- \to Zh) \times \mathcal{B}(h \to WW^*)$ *(lower row) for the lightest* $\mathcal{CP}$*-even CMSSM Higgs boson, normalized to the value in the SM with the same Higgs mass, are given in the* $(M_A, m_0)$ *planes for* $\mu > 0$ *and the values of* $\tan\beta$ *and* $A_0$ *specified in the plots. The dot-dashed (orange) line represents the border of the CMSSM parameter space. The other contours and shadings are the same as in Fig. 1.*

check of both the CMSSM and the NUHM.

The situation at the $\gamma$C is somewhat worse than at the LC. Only for small $\tan\beta = 10$ can indirect limits on $M_A$ be obtained. In the $h \to b\bar{b}$ channel, limits of $M_A \lesssim 900$ (500) GeV can be derived at the 1–2$\sigma$ level. Using the $h \to WW^*$ channel, corresponding limits of 700 (500) GeV might be possible. Improved sensitivity could be obtained by combining LC and $\gamma$C results, but such a combination goes beyond the scope of this paper.

The analysis above demonstrates that the sensitivity of the Higgs sector observables to variations in $M_A$ can be useful for testing the universality assumption of the CMSSM, i.e. for distinguishing between the CMSSM and the NUHM. In order to investigate this issue in more detail, we focus on the NUHM scenario presented in Fig. 1 of [20], in which $m_{1/2} = 300$ GeV, $m_0 = 100$ GeV, $\tan\beta = 10$ and $A_0 = 0$ were chosen. For this choice of parameters, consistent models require $M_A \gtrsim 200$ GeV and $|\mu| \lesssim 650$ GeV,

We show in Fig. 8 the values of $\sigma \times \mathcal{B}$ (as before, normalized to the SM value) obtained by varying either $M_A$ or $\mu$ around the CMSSM point. The upper row shows the variations with $M_A$, which may be substantial, particularly in the $h \to b\bar{b}$ and $h \to WW^*$ channels at the LC. The variations at the $\gamma$C are somewhat smaller, and those at the $\mu$C could be larger (though this information will presumably be available only on a longer time scale). In the case of the LC, the deviation from the CMSSM prediction (for which $M_A = 440$ GeV) could be as large as $\sim -2.5(+1.5)\sigma$ or more in the $h \to WW^*$ channel for $\delta M_A = -(+)100$ GeV. The $h \to b\bar{b}$ channel is somewhat less sensitive, with deviations of $\sim +1.5(-0.8)\sigma$ for the same range of $\delta M_A$. Thus, this key parameter of the MSSM Higgs boson sector, which we recall is difficult to observe in this mass range, might be determined indirectly within the framework of the NUHM. This would provide a possibily for distinguishing between the CMSSM and the NUHM, even in the case where no direct information on $M_A$ is available.

The variation with $\mu$ (which in contrast to $M_A$ enters the Higgs sector observables only at loop level), as shown in the lower part of Fig. 8, is much smaller than the $M_A$ variation. The deviations from the CMSSM point of $\mu = 390$ GeV barely exceed $1\sigma$ for all channels over the entire parameter space. Therefore, in a scenario with relatively small $\tan\beta$, no substantial limits on $\mu$ can be inferred from a precise measurement of the $\sigma \times \mathcal{B}$ observables, and one has to rely on direct measurements. In the case of $\mu$, this will most likely be possible due to measurements in the gaugino sector of the MSSM [37].

# 5 Conclusions

Extending our previous work on hadron colliders, we have analyzed in this paper the abilities of $e^+e^-$, $\gamma\gamma$ and $\mu^+\mu^-$ colliders to constrain MSSM parameters indirectly via accurate measurements of the production and decays of the lightest $\mathcal{CP}$-even MSSM Higgs boson. We have estimated the numbers of standard deviations by which $e^+e^-$, $\gamma\gamma$ and $\mu^+\mu^-$ measurements might differ from their SM values, and shown how these sensitivities vary with the CMSSM parameters $m_{1/2}, m_0, \tan\beta$ and $A_0$. We have shown that this information is potentially complementary to that provided by direct searches for MSSM particles, as well as the indirect constraints provided by $b \to s\gamma$ decay, $g_\mu - 2$, and cosmology.

In particular, we have shown that $e^+e^-$, $\gamma\gamma$ and $\mu^+\mu^-$ measurements might be able to constrain the mass of the $\mathcal{CP}$-odd MSSM Higgs boson if it remains undetected at the LHC or the LC. We have discussed the impact of the indirect information on $M_A$ both within

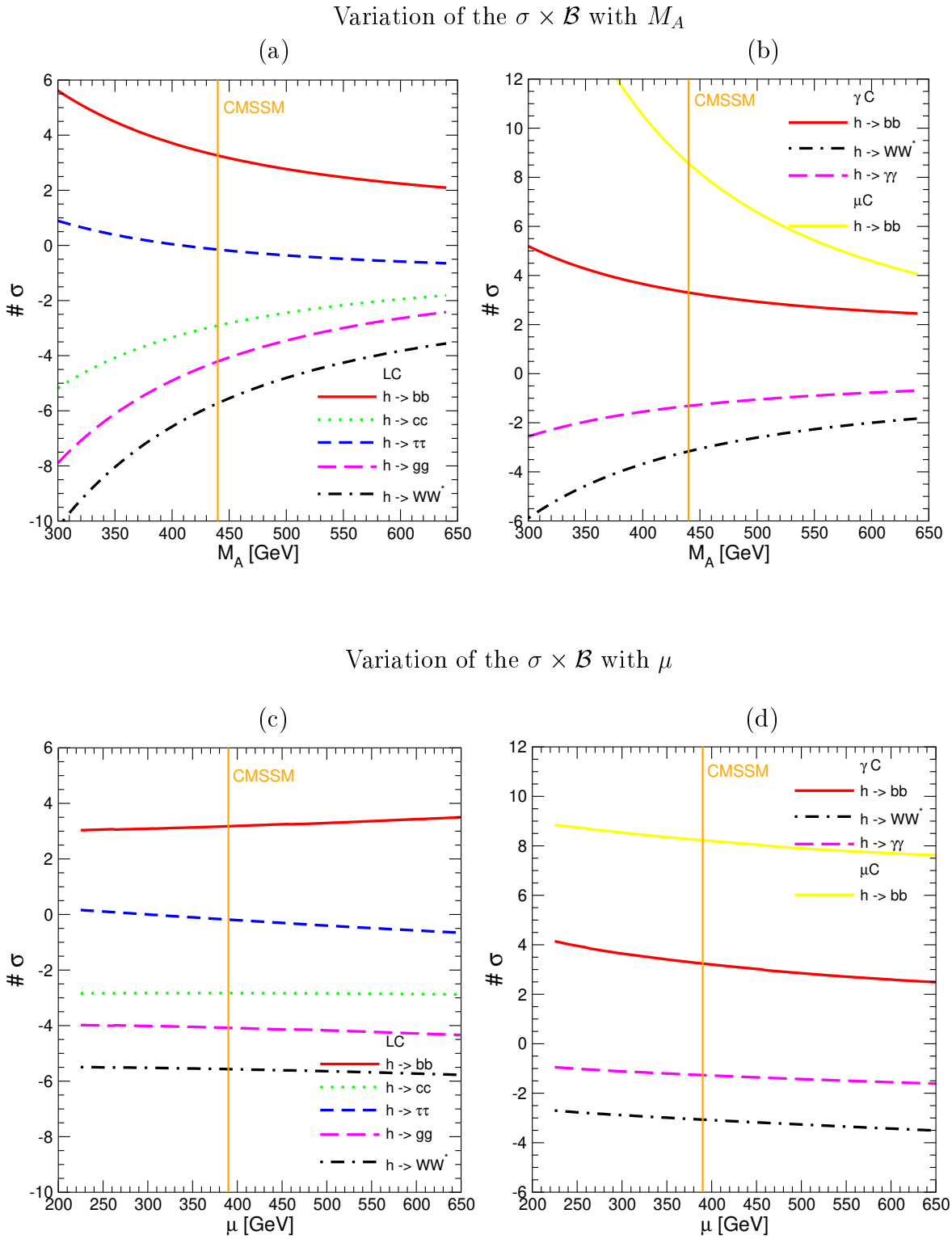


Figure 8: *The numbers of standard deviations of the predictions in the NUHM as compared to the SM are shown in the different $\sigma \times \mathcal{B}$ channels for the LC (left column) and the $\gamma C$ and $\mu C$ (right column) as functions of $M_A$ (upper row) and $\mu$ (lower row). The corresponding CMSSM values of $M_A$ and $\mu$ are indicated by light vertical (orange) lines. The other parameters have been chosen as $m_{1/2} = 300$ GeV, $m_0 = 100$ GeV, $\tan\beta = 10$ and $A_0 = 0$.*

the framework of the CMSSM (where the mass of the $\mathcal{CP}$-odd MSSM Higgs boson is related to the CMSSM parameters $m_{1/2}, m_0, \tan\beta$ and $A_0$), and in the NUHM (in which the soft supersymmetry-breaking masses of the MSSM Higgs multiplets are allowed to differ from those of the squarks and sleptons). A direct observation of the $\mathcal{CP}$-odd MSSM Higgs boson, on the other hand, would enable stringent consistency tests both of the CMSSM and the NUHM.

We have furthermore demonstrated in this context that $e^+e^-$, $\gamma\gamma$ and $\mu^+\mu^-$ measurements are sensitive to deviations between the CMSSM and the NUHM, i.e. they allow one to test the universality assumption of the CMSSM. This refers in particular to deviations arising from changing $M_A$ compared to its CMSSM value, while the sensitivities to deviations from the CMSSM value of $\mu$, which enters the Higgs sector observables only via loop corrections, are less promising.

We have emphasized in this paper the role of the Higgs-sector observables and the indirect constraints from $b \to s\gamma$, $g_\mu - 2$, and cosmology for testing supersymmetric models. In a realistic scenario one would of course seek to combine this information with that obtained from the possible observation of a spectrum of supersymmetric particles, taking into account all available results from different colliders. On the basis of the combined information obtained in this way one would then try to disentangle the detailed structure of supersymmetry breaking.

The analysis performed in this paper, in which we have investigated the sensitivity to deviations between two particular models, the CMSSM and the NUHM, is a step into this direction, but there is clearly more work needed along those lines. This could for instance involve a more detailed exploration of the NUHM as well as models beyond the NUHM, e.g., by relaxing further the universality assumptions for the soft supersymmetry-breaking masses of squarks and sleptons. We believe that this paper lays the basis for such further studies, by quantifying the abilities of different colliders to constrain indirectly MSSM parameters that may be difficult to measure directly at the LHC, or even at a LC. Further work on the capabilities of $e^+e^-$, $\gamma\gamma$ and $\mu^+\mu^-$ measurements to test supersymmetric models is clearly in order to be prepared for the many different possibilities in which supersymmetry might manifest itself in nature.

## Acknowledgments

The work of K.A.O. was partially supported by DOE grant DE–FG02–94ER–40823. This work has been supported by the European Community's Human Potential Programme under contract HPRN-CT-2000-00149 Physics at Colliders.

# References

[1] J. Ellis, S. Heinemeyer, K. Olive and G. Weiglein, *Phys. Lett.* **B 515** (2001) 348, hep-ph/0105067.

[2] S. Ambrosanio, A. Dedes, S. Heinemeyer, S. Su and G. Weiglein, *Nucl. Phys.* **B 624** (2001) 3, hep-ph/0106255.

[3] R. Harlander and W. Kilgore, *Phys. Rev. Lett.* **88** (2002) 201801, hep-ph/0201206;
C. Anastasiou and K. Melnikov, hep-ph/0207004.

[4] M. Battaglia et al., *Eur. Phys. J.* **C 22** (2001) 535, hep-ph/0106204.

[5] T. Hahn, S. Heinemeyer and G. Weiglein, hep-ph/0211204.

[6] TESLA TDR Part 3: *Physics at an $e^+e^-$ Linear Collider*, eds. R.D. Heuer, D. Miller, F. Richard and P.M. Zerwas, hep-ph/0106315, see: `http://tesla.desy.de/tdr` .

[7] J. Brient, talk at the Linear Collider Workshop, Cracow, Poland, September 2001, see: `http://webnt.physics.ox.ac.uk/lc/ecfadesy`.

[8] TESLA TDR Part 6, Chapter 1: *Photon collider at TESLA*, hep-ex/0108012, see: `http://tesla.desy.de/tdr` .

[9] D. Asner et al., hep-ex/0111056.

[10] C. Blöchinger et al., Higgs factory working group of the ECFA-CERN study on Neutrino Factory & Muon Storage Rings at CERN, *Physics opportunities at $\mu^+\mu^-$ Higgs factories*, hep-ph/0202199.

[11] S. Heinemeyer, W. Hollik and G. Weiglein, *Eur. Phys. Jour.* **C 16** (2000) 139, hep-ph/0003022.

[12] A. Djouadi, J. Kalinowski and M. Spira, *Comput. Phys. Commun.* **108** (1998) 56, hep-ph/9704448.

[13] Particle Data Group, K. Hagiwara et al., *Phys. Rev.* **D 66** (2002) 010001.

[14] LEP Higgs working group, LHWG Note/2002-01,
`http://lephiggs.web.cern.ch/LEPHIGGS/papers/`.

[15] M. Alam et al. [CLEO Collaboration], *Phys. Rev. Lett.* **74** (1995) 2885, as updated in S. Ahmed et al., CLEO CONF 99-10;
[Belle Collaboration], BELLE-CONF-0003, contribution to the 30th International conference on High-Energy Physics, Osaka, 2000. See also
K. Abe et al. [Belle Collaboration], hep-ex/0103042;
K. Abe *et al.*, [Belle Collaboration], hep-ex/0107065;
L. Lista [BaBar Collaboration], hep-ex/0110010.

[16] G. Degrassi, P. Gambino and G. F. Giudice, *JHEP* **0012** (2000) 009, hep-ph/0009337;
M. Carena, D. Garcia, U. Nierste and C. E. Wagner, *Phys. Lett.* **B 499** (2001) 141, hep-ph/0010003;
D. Demir and K. Olive, *Phys. Rev.* **D 65** (2002) 034007, hep-ph/0107329.

[17] H. Brown et al. [Muon $g_\mu - 2$ Collaboration], *Phys. Rev. Lett.* **86** (2001) 2227, hep-ex/0102017;
G. Bennett et al. [Muon $g_\mu - 2$ Collaboration], *Phys. Rev. Lett.* **89** (2002) 101804 [Erratum-ibid. **89** (2002) 129903], hep-ex/0208001.

[18] J. Ellis, J. Hagelin, D. Nanopoulos, K. Olive and M. Srednicki, *Nucl. Phys.* **B 238** (1984) 453; see also
H. Goldberg, *Phys. Rev. Lett.* **50** (1983) 1419.

[19] A. Melchiorri and J. Silk, *Phys. Rev.* **D 66** (2002) 041301, astro-ph/0203200.

[20] J. Ellis, K. Olive and Y. Santoso, *Phys. Lett.* **B 539** (2002) 107, hep-ph/0204192.

[21] S. Heinemeyer, W. Hollik and G. Weiglein, *Comput. Phys. Commun.* **124** (2000) 76, hep-ph/9812320; hep-ph/0002213; the `FeynHiggs` code is available from `http://www.feynhiggs.de`.

[22] S. Heinemeyer, W. Hollik and G. Weiglein, *Phys. Rev.* **D 58** (1998) 091701, hep-ph/9803277; *Phys. Lett.* **B 440** (1998) 296, hep-ph/9807423; *Eur. Phys. Jour.* **C 9** (1999) 343, hep-ph/9812472.

[23] G. Degrassi, S. Heinemeyer, W. Hollik, P. Slavich and G. Weiglein, *in preparation.*

[24] M. Frank, S. Heinemeyer, W. Hollik and G. Weiglein, hep-ph/0202166.

[25] A. Brignole, G. Degrassi, P. Slavich and F. Zwirner, *Nucl. Phys.* **B 631** (2002) 195, hep-ph/0112177.

[26] A. Brignole, G. Degrassi, P. Slavich and F. Zwirner, *Nucl. Phys.* **B 643** (2002) 79, hep-ph/0206101.

[27] J. Ellis, T. Falk, G. Ganis, K. Olive and M. Srednicki, *Phys. Lett.* **B 510** (2001) 236, hep-ph/0102098.

[28] M. Knecht and A. Nyffeler, *Phys. Rev.* **D 65** (2002) 073034, hep-ph/0111058;
M. Knecht, A. Nyffeler, M. Perrottet and E. De Rafael, *Phys. Rev. Lett.* **88** (2002) 071802, hep-ph/0111059;
I. Blokland, A. Czarnecki and K. Melnikov, *Phys. Rev. Lett.* **88** (2002) 071803, hep-ph/0112117;
M. Ramsey-Musolf and M. Wise, *Phys. Rev. Lett.* **89** (2002) 041601, hep-ph/0201297.

[29] M. Davier, S. Eidelman, A. Hocker and Z. Zhang, hep-ph/0208177.

[30] K. Hagiwara, A. Martin, D. Nomura and T. Teubner, hep-ph/0209187;
F. Jegerlehner, unpublished, as reported in M. Krawczyk, hep-ph/0208076.

[31] A. Benoit et al. [Archeops Collaboration], astro-ph/0210306.

[32] ATLAS Collaboration, *Detector and Physics Performance Technical Design Report*, CERN/LHCC/99-15 (1999), see:
`atlasinfo.cern.ch/Atlas/GROUPS/PHYSICS/TDR/access.html` .

[33] D. Cavalli et al., [Les Houches Higgs working group], *Summary report*, hep-ph/0203056.

[34] K. Babu and C. Kolda, *Phys. Lett.* **B 451** (1999) 77, hep-ph/9811308;
M. Battaglia and K. Desch, hep-ph/0101165;
S. Heinemeyer and G. Weiglein, hep-ph/0102117;
J. Guasch, W. Hollik and S. Peñaranda, *Phys. Lett.* **B 515** (2001) 367, hep-ph/0106027;
M. Carena, H. Haber, H. Logan and S. Mrenna, *Phys. Rev.* **D 65** (2002) 055005, hep-ph/0106116;
A. Curiel, M. Herrero, D. Temes and J. De Troconiz, *Phys. Rev.* **D 65** (2002) 075006, hep-ph/0106267;
S. Dawson and S. Heinemeyer, *Phys. Rev.* **D 66** (2002) 055002, hep-ph/0203067.

[35] J. Erler, S. Heinemeyer, W. Hollik, G. Weiglein and P.M. Zerwas, *Phys. Lett.* **B 486** (2000) 125, hep-ph/0005024.

[36] J. Ellis, T. Falk, K. Olive and Y. Santoso, hep-ph/0210205.

[37] S. Choi, J. Kalinowski, G. Moortgat-Pick and P. Zerwas, *Eur. Phys. J.* **C 22** (2001) 563, hep-ph/0108117; hep-ph/0202039.